Comparing Gas Adsorbates for Pore-Structure Characterization of Nanoporous Materials

1. Background

Nanoporous materials such as zeolites, activated carbons, and metal–organic frameworks (MOFs) feature abundant microporosity and play central roles in adsorption, catalysis, and separations.[1,2] Accurately resolving pore size distributions, micropore volumes, and accessible surface areas is therefore essential for materials design and process modeling. Gas physisorption remains the primary technique for this purpose because it probes adsorption–desorption behavior over a wide relative-pressure window spanning low pressures (below 0.1 Pa) through saturation near the adsorbate's boiling point.[3] Reliable measurements in this regime require high vacuum instrumentation capable of evacuating the manifold and sample cell to very low absolute pressures with stable temperature control.

Micropore filling at low P/P_0 is well described by Polanyi potential theory, where adsorption in ultramicropores (widths $\lesssim 0.7$ nm, i.e., only two to three molecular diameters) occurs via overlapping dispersion fields, often termed 'primary micropore filling.' As pore width increases, adsorbate–adsorbate interactions contribute more strongly and filling proceeds at higher relative pressures ('secondary filling'). The choice of probe molecule and temperature strongly affects the apparent filling pressure, diffusional kinetics, and potential specific interactions with surface functional groups; consequently, N_2 (77 K), Ar (87 K), and CO_2 (195 K and 273 K) are commonly used in a complementary manner to resolve the full micropore/mesopore range.[4,5]

This note compares N_2 (77 K), Ar (87 K), and CO_2 (195 K, 273 K) for three representative materials—zeolite, activated carbon, and a MOF—and shows how combining probes yields a more complete and kinetically reliable description of the pore structure.

2. Experiment

Low-temperature N_2 (77 K) adsorption–desorption isotherms were collected on an **AMI Micro 300C** static volumetric analyzer, which is equipped with a turbo molecular pump (up to 10^{-8} Pa). For sub-boiling cryogenic control, auxiliary devices stabilized Ar at 87 K and CO_2 at 195 K with liquid-nitrogen cooling of the transfer medium. A water bath provided precise control for CO_2 at 273 K.

N_2 (77 K) and Ar (87 K) were measured across wide P/P_0 ranges from $\leq 10^{-7}$ to near 1, capturing primary/secondary micropore filling and mesopore capillary condensation. Micropore pore size distributions (PSDs) were derived using HK-SF models for consistency across probes. CO_2 (273 K) was measured up to $P/P_0 \approx 3\times10^{-2}$ Pa to resolve ultranarrow micropores (<~1 nm) with high diffusion rates. CO_2 (195 K) extended the range to $P/P_0 \rightarrow 1$ for assessing 1–2 nm pores and total pore volume. Samples. A representative zeolite, activated carbon, and MOF were evaluated under each probe condition.

3. Results

3.1 N_2 (77 K) vs. Ar (87 K): Micropore Resolution and Kinetics

For zeolite, activated carbon, and MOF, both N_2- and Ar-based isotherms exhibit Type-I behavior (shown in Figures 1–3a), confirming dominant microporosity and strong adsorbent–adsorbate interactions. In the low-pressure regime, the initial filling with Ar occurs at higher P/P_0 ($\approx 10^{-5}$) than with N_2 ($\approx 10^{-7}$). Despite this shift, HK-SF micropore PSDs derived from N_2 and Ar agree closely across all three materials (Figures 1–3c,d), indicating that Ar at 87 K can recover the same pore size information while offering faster equilibration and reduced quadrupole-induced artifacts on polar surfaces.

When materials contain polar functional groups or exposed ions, Ar (87 K) minimizes orientation effects that can bias N_2 uptake at 77 K and can shorten run time by accelerating equilibrium. For purely carbonaceous materials, N_2 at 77 K remains effective, but complementary Ar measurements are valuable when sub-nanometer features are critical.

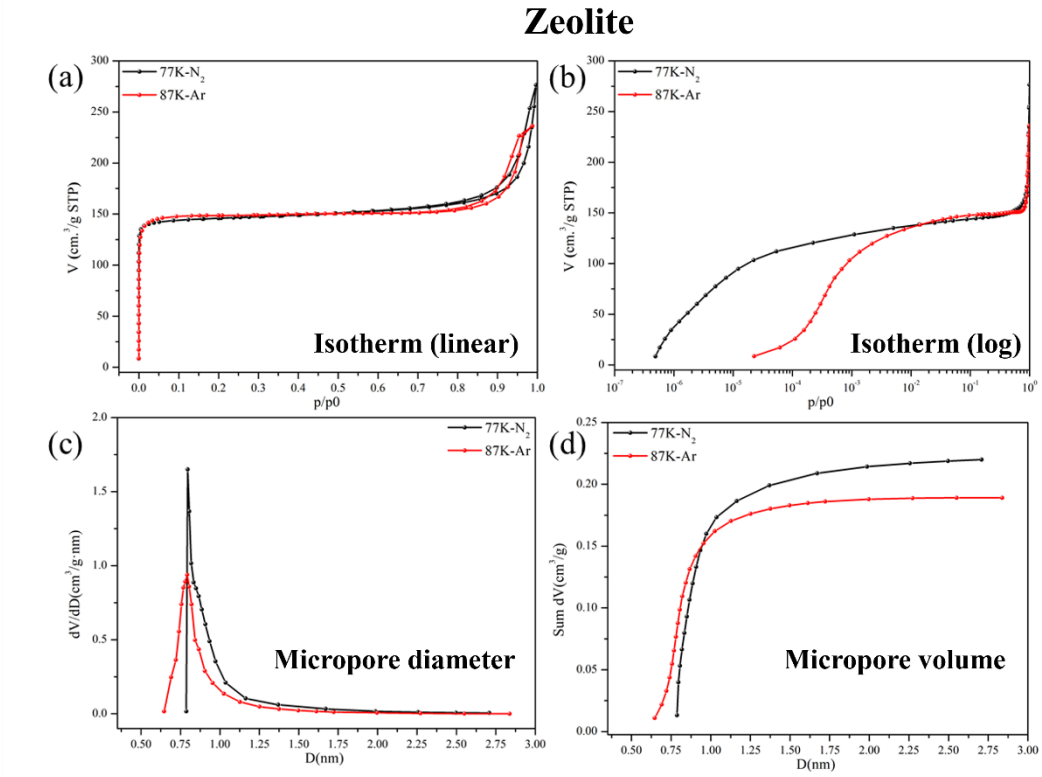

Figure 1: a) Zeolite N_2 and Ar gas adsorption and desorption curves (linear coordinates); b) zeolite N_2 and Ar gas adsorption desorption curves (logarithmic coordinates); c) HK-SF micropore size distribution; d) HK-SF micropore volume distribution

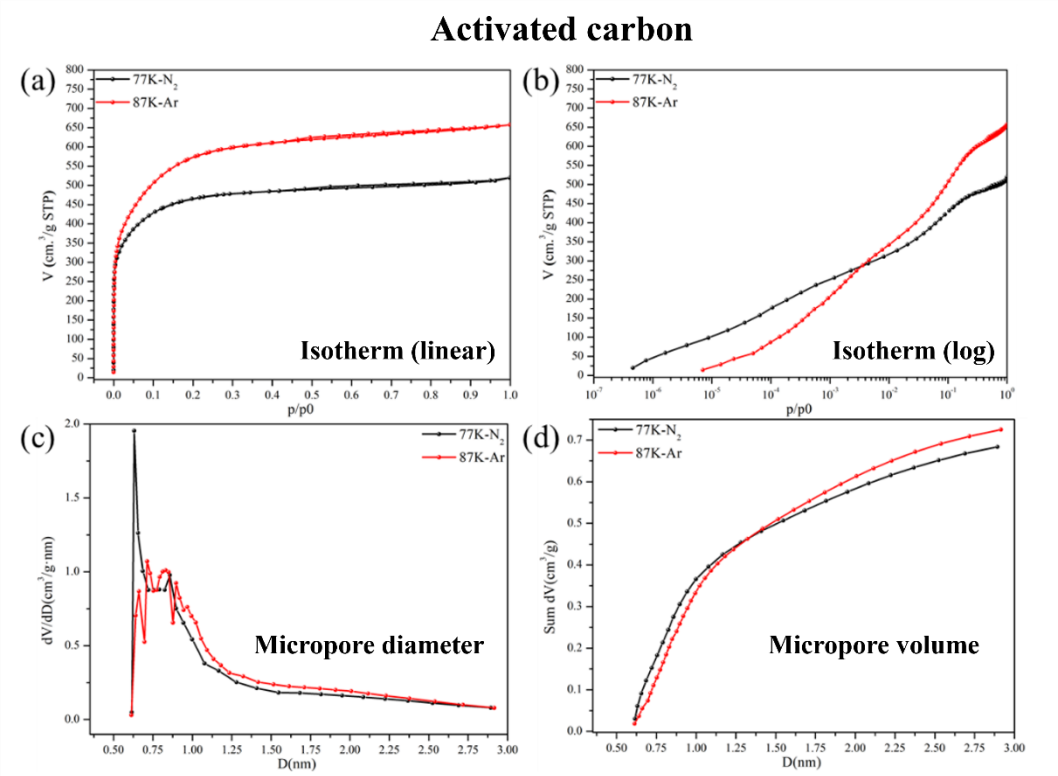

Figure 2: a) Activated carbon N_2 and Ar gas adsorption and desorption curves (linear coordinates); b) activated carbon N_2 and Ar gas adsorption desorption curves (logarithmic coordinates); c) HK-SF micropore size distribution; d) HK-SF micropore volume distribution

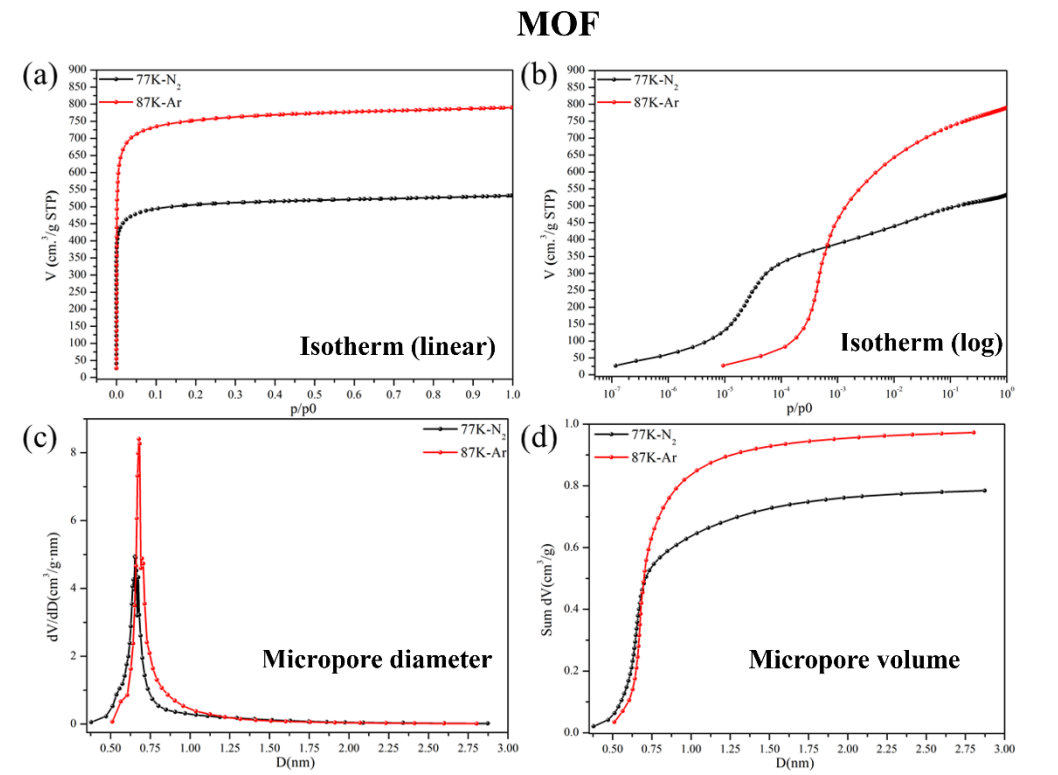

Figure 3: a) MOF N_2 and Ar gas adsorption and desorption curves (linear coordinates); b) MOF N_2 and Ar gas adsorption desorption curves (logarithmic coordinates); c) HK-SF micropore size distribution; d) HK-SF micropore volume distribution

3.2 CO_2 (273 K, 195 K): Ultranarrow Pores and Total Microporosity

For activated carbon, CO_2 (273 K) yields a lower saturation capacity at 100 kPa than N_2 at 77 K (Figure 4a–b), reflecting the higher temperature and the limited accessible P/P_0 ($\leq 3\times10^{-2}$) at ambient pressure. Within this window, CO_2 probes pores down to ~0.4 nm, delivering high-resolution ultramicropore information that is kinetically difficult to obtain with N_2 or even Ar at cryogenic temperatures.

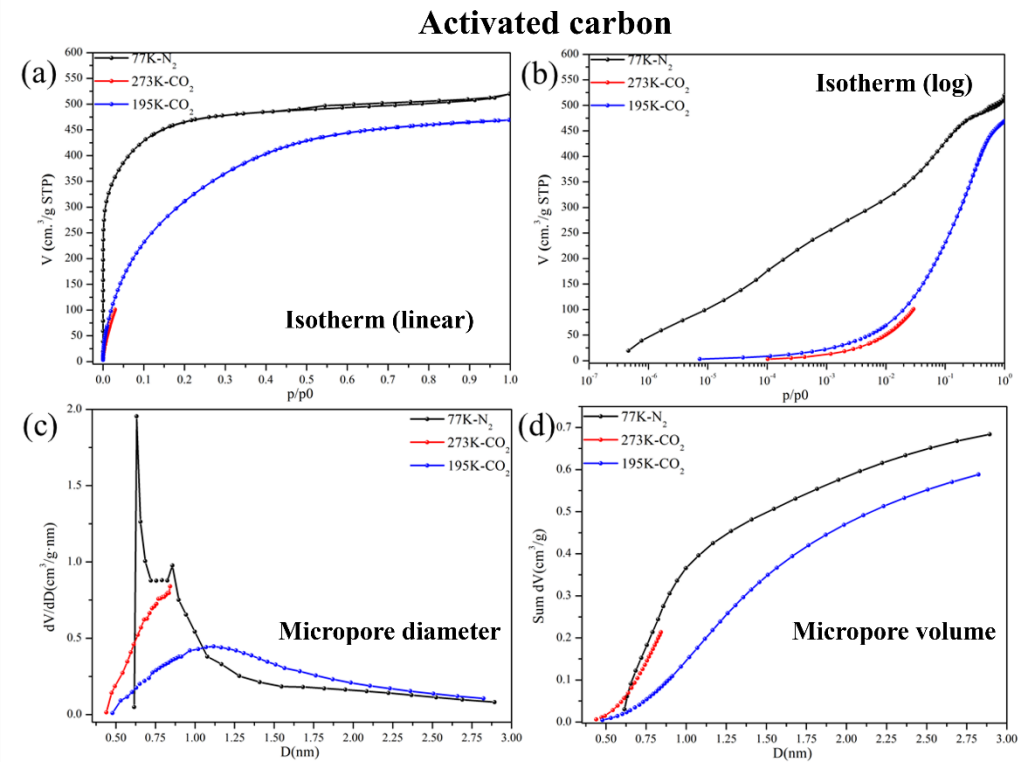

Figure 4: a) Activated carbon N_2, Ar, and CO_2 (195 K) gas adsorption and desorption curves (linear coordinates); b) activated carbon N_2, Ar, and CO_2 (195 K) gas adsorption desorption curves (logarithmic coordinates); c) HK-SF micropore size distribution; d) HK-SF micropore volume distribution

Lowering the CO_2 temperature to 195 K dramatically extends the analysis range. The isotherm reaches $P/P_0 \rightarrow 1$, enabling both ultramicropore (<1 nm) and 1–2 nm micropore characterization and estimation of total pore volume, which are capabilities that CO_2 (273 K) lacks. Similar trends are observed for zeolite and the MOF (Figures 5–6). CO_2 (195 K) shows strong Type-I behavior with saturation capacities exceeding 273 K and PSDs that align well with those derived from N_2 (77 K) and Ar (87 K) across the <2 nm regime.

Although CO_2's small size and rapid diffusion are advantageous for ultramicropores, its larger quadrupole (compared to N_2) can lead to specific interactions on polar surfaces. For such materials, cross-validating CO_2-based PSDs with Ar (87 K) is recommended.

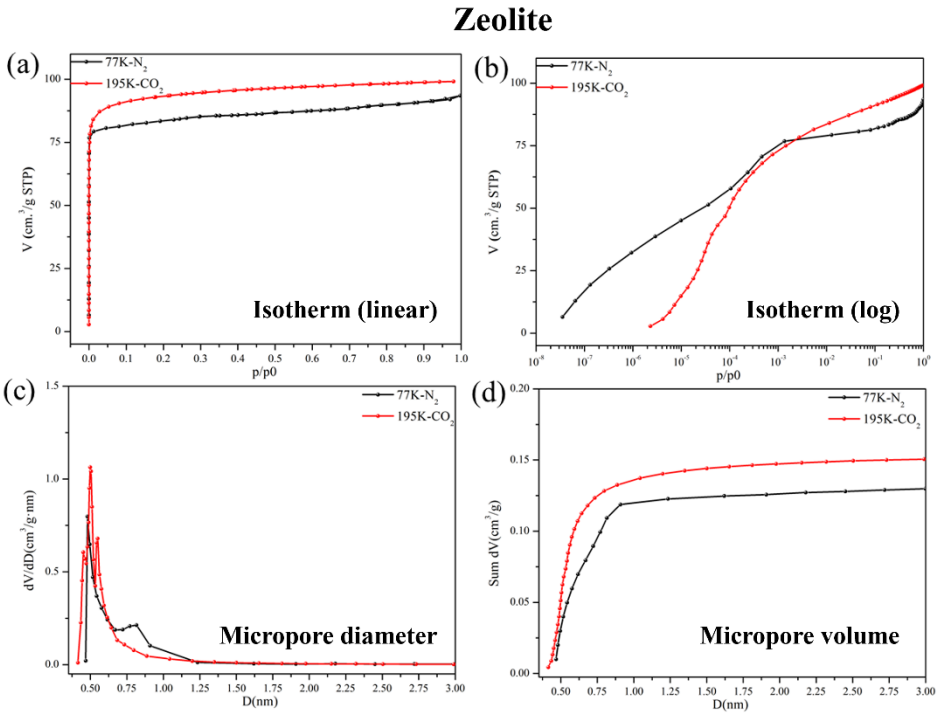

Figure 5: a) Zeolite N_2 and CO_2 (195 K) gas adsorption and desorption curves (linear coordinates); b) zeolite N_2 and CO_2 (195 K) gas adsorption desorption curves (logarithmic coordinates); c) HK-SF micropore size distribution; d) HK-SF micropore volume distribution

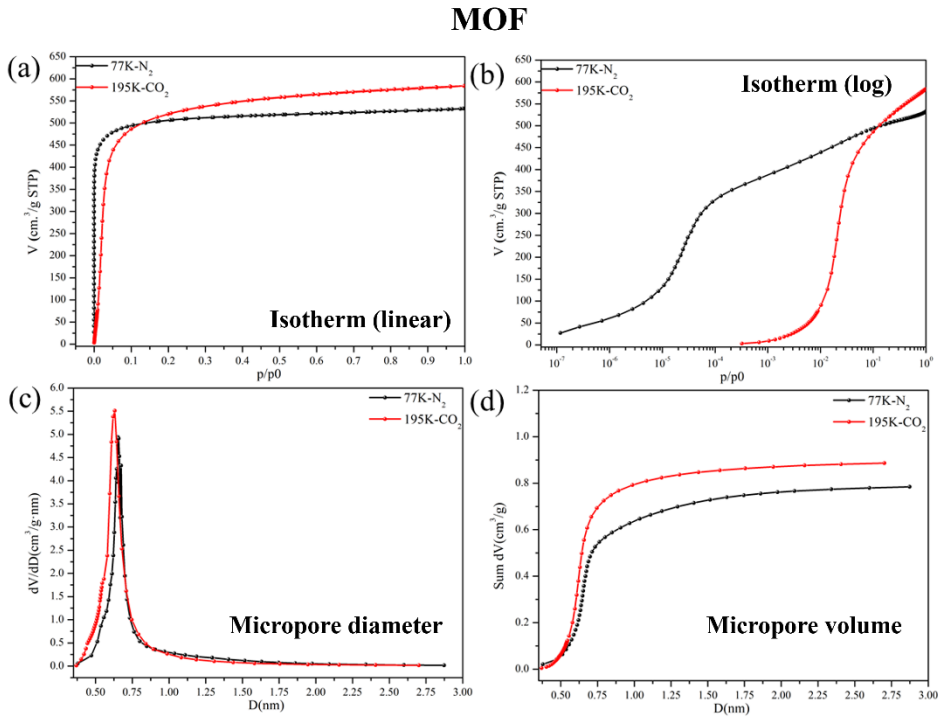

Figure 5: a) MOF N_2 and CO_2 (195 K) gas adsorption and desorption curves (linear coordinates); b) MOF N_2 and CO_2 (195 K) gas adsorption desorption curves (logarithmic coordinates); c) HK-SF micropore size distribution; d) HK-SF micropore volume distribution

4. Conclusions

Using N_2 (77 K), Ar (87 K), and CO_2 (195 K and 273 K) in a complementary fashion provides a complete and kinetically reliable picture of microporosity in zeolites, activated carbons, and MOFs. Ar (87 K) improves equilibration and reduces quadrupole-related artifacts relative to N_2, but the PSD plots are still comparable to N_2 (77 K). CO_2 (273 K) resolves ultranarrow pores with fast diffusion but limited P/P_0 range, while CO_2 (195 K) extends analysis to ~2 nm and enables total micropore volume determination.

*Figure 7: Highlighted features of **Micro 300C** physisorption analyzer from **AMI***

The **AMI Micro 300C** shown in Figure 7, equipped with a turbo molecular pump, provides the optimal platform for low-pressure adsorption-desorption experiments. The turbo-backed, ultra-high-vacuum manifold minimizes residual gases and dead-volume effects, enabling stable baselines and accurate isotherms from the ultra-low-pressure regime through near-saturation. The **Micro 300C** offers tightly controlled temperature staging (for pre-activation, absorption, and desorption) which shortens equilibration and improves repeatability across alloys, modified surfaces, and cycling protocols. Equally important, **Micro 300C** data aligns seamlessly with complementary **AMI** systems like the **RuboSorp MPA** for high-pressure capacity and the **RuboSorp MSB** for high-resolution gravimetric kinetics. Exceptional sensitivity, vacuum purity, and cross-platform consistency make the **AMI Micro 300C** ideal for routine QA/QC and advanced R&D on solid-state porous materials.

5. References

(1) Thommes, M. and Schlumberger, C. Characterization of nanoporous materials. *Annu. Rev. Chem. Biomol. Eng.* **2021**, *12*, 137-162.
(2) Kianfar, E. and Sayadi, H. Recent advances in properties and applications of nanoporous materials and porous carbons. *Carbon Lett*. **2022**, *32*, 1646-1669.
(3) Thommes, M.; Kaneko, K.; Neimark, A. V.; Olivier, J. P.; Rodriguez-Reinoso, F.; Rouquerol, J.; Sing, K. S. W. Physisorption of gases, with special reference to the evaluation of surface area and pore size distribution (IUPAC Technical Report). *Pure Appl. Chem.* **2015**, *87*, 1050-1069.
(4) Beda, A.; Vaulot, C.; Ghimbeu, C. M. Hard carbon porosity revealed by the adsorption of multiple gas probe molecules (N_2, Ar, CO_2, O_2 and H_2). *J. Mater. Chem. A*, **2021**, *9*, 937-943.
(5) Kim, K. H. and Kim, M. H. Adsorption of CO_2, CO, H_2, and N_2 on zeolites, activated carons, and metal-organic frameworks with different surface nonuniformities. *Sustainability*, **2023**, *15*, 11574.